Metal Binding by Humic Substances – Characterization by High-Resolution Lanthanoide Ion Probe Spectroscopy (HR-LIPS)

Bettina Marmodée[a], Joost de Klerk[b], Freek Ariese[b], Cees Gooijer[b], and Michael U. Kumke[a]

[a] Institute of Chemistry, University of Potsdam, Karl-Liebknecht-Straße 24 – 25, D-14476 Potsdam-Golm, Germany
[b] Department of Analytical Chemistry and Applied Spectroscopy, Vrije Universiteit, De Boelelaan 1083, NL-1081 HV Amsterdam, The Netherlands

Reprint requests to PD Dr. M. U. K.; Fax: +49 331 9775058; E-mail: kumke@chem.uni-potsdam.de

Z. Naturforsch. **64a,** 242 – 250 (2009); received September 19, 2008

In ultra-low-temperature experiments at 4.7 K the luminescence of Eu(III) bound to different hydroxy- and methoxybenzoic acids and to humic substances (HS) was investigated. The benzoic acid derivatives were used as simple model compounds for common metal-binding structures in HS. The Eu(III) luminescence was directly excited by means of a pulsed dye laser, scanning through the $^5D_0 \leftarrow {}^7F_0$ transition of Eu(III) and subsequently high-resolution total luminescence spectra (TLS) were recorded. Based on the thorough analysis of the high-resolution TLS conclusions were drawn with respect to the number of different complexes formed and to the symmetry of the complexes. The crystal-field strength parameter $N_v(B_{2q})$ was dependent on the electrostatic forces induced by the ligands as well as on the symmetry of the complexes. The formation of thermodynamically stable complexes was found to be slow even for small model ligands such as 2-hydroxybenzoic acid. Comparison between the model compounds and HS clearly revealed that the carboxylate group is the dominant binding site in HS. Indices for the formation of chelates, e. g. similar to 2-hydroxybenzoic acid, were not found for HS.

Key words: Humic Substances; Europium; Benzoic Acids; Low-Temperature Luminescence.

1. Introduction

The bioavailability and subsequently the toxicity and fate of metal ions is, to a large extent, determined by their speciation [1 – 5]. Transport and distribution of heavy metals in the environment depend on the speciation. Consequently speciation is a key issue and has to be examined thoroughly, for instance in order to evaluate the suitability of waste disposal sites or the danger emanating from accidents involving heavy metals or radionuclides. Knowledge regarding the transport and immobilization processes of radionuclides in the near and far field of nuclear waste repository sites is a central issue in long-term safety assessments of such sites [6]. For the speciation of metal ions in the environment, especially in soil and water, humic substances (HS) play a key role [7, 8]. Due to the presence of ionic or highly dipolar functional groups (mainly carboxylic and phenolic groups, but also N-containing moieties), HS form strong complexes with metal ions and hence HS subsequently determine the speciation of the metal ions in the environment [7, 9, 10]. For these reasons, the characterization of the HS-metal complexes and the understanding of processes involved in the complexation by HS is of utmost importance for a reliable modelling of the ecological risks of metal ions.

For in-situ sensing applications based on spectroscopy the understanding of the basic photophysical parameters is indispensable. The complexation of metal ions can be monitored using spectroscopic methods, e. g., measuring the quenching of the intrinsic HS fluorescence to describe qualitatively and quantitatively the metal binding by HS [11]. However, the fluorescence properties of HS are very complex and interpretation is hampered by the extremely inhomogeneous nature of HS, e. g., even under cryogenic conditions ($T < 10$ K) only broadbanded spectra are observed [12]. Therefore, the use of external luminescence probes such as europium [Eu(III)] or terbium [Tb(III)] ions is a promising alternative for the in-depth investigation of metal complexation by HS. Moreover, Eu(III) is a natural analogue of actinoides [An(III)], which makes it very attractive as a surrogate in the investigation of actinoide migra-

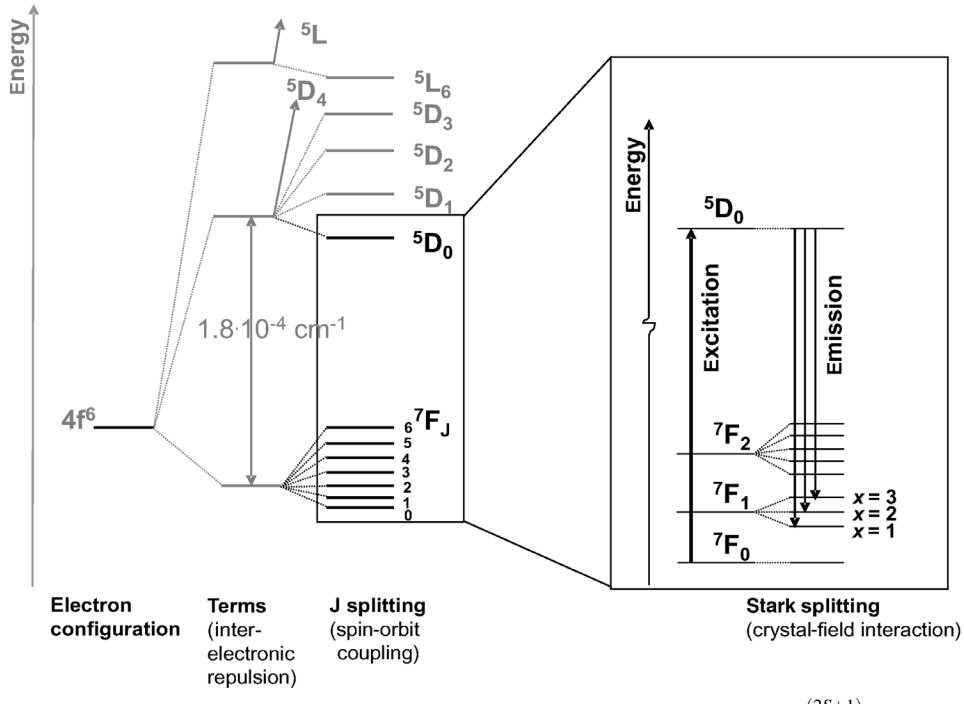

Fig. 1. Energy scheme of the free Eu(III) ion (according to [14]) and Stark splitting of the $^{(2S+1)}L_J$ levels, if Eu(III) is surrounded by a crystal-field. Only the $^5D_0 \rightarrow {}^7F_1$ emission is shown.

tion in the environment (e. g., in geological barriers of nuclear waste repository sites). Because of its outstanding luminescence properties, it can be used to probe the molecular environment in metal-HS complexes [13, 14]. The observed spectral features as well as the luminescence decay time of Eu(III) are directly correlated with the complex formed. Depending on the experimental set up, information about the stoichiometry, geometry and stability of the complex can be obtained [13]. In room-temperature measurements complexation constants have been derived from the sensitized Eu(III) emission and from changes in the ratio of the Eu(III) luminescence bands ($^5D_0 \rightarrow {}^7F_1$ and $^5D_0 \rightarrow {}^7F_2$) [15 – 17]. Because of the very low extinction coefficients of Eu(III) at most wavelengths, excitation is often carried out at $\lambda_{ex} = 395$ nm, which corresponds to the strongest transition in the UV/Vis spectral range, with an extinction coefficient ε_{395nm} of about 3 M^{-1} cm^{-1} [18], or indirectly via energy transfer from the ligands (making use of the so-called antenna effect). Yoon *et al.* [19] used direct $^5D_0 \leftarrow {}^7F_0$ excitation (see Fig. 1) to gain information on the number of different Eu(III) complexes formed with HS. Since this transition is non-degenerate and thus not split by the crystal-field (Stark splitting), its energy is characteristic for a specific complex [20]. In the present study this transition was probed using an alternative approach: fluorescence line-narrowing (FLN) spectroscopy [21]. High-resolution luminescence spectra were recorded at ultra-low temperatures (4.7 K), making use of energy-selective excitation by a narrow-banded, tuneable dye laser. It has been reported that under such conditions additional information on the interaction of HS with xenobiotics becomes accessible [22]. In the present paper FLN spectroscopy is used to study Eu(III)/(model ligands) and Eu(III)-HS complexes. A major difference to FLN studies of molecular systems is, that rather than probing vibronic bands of the same electronic transition, now different electronic transitions are used for excitation and emission. Nevertheless, the energies of these inhomogeneously broadened transitions were found to be correlated, and line-narrowing was observed. As will be shown below, the reduction of the inhomogeneous band width enables a rather precise determination of energy splittings of the $^7F_1$ multiplet and thus the crystal-field strength parameter can be derived. On this basis, information about the number of different

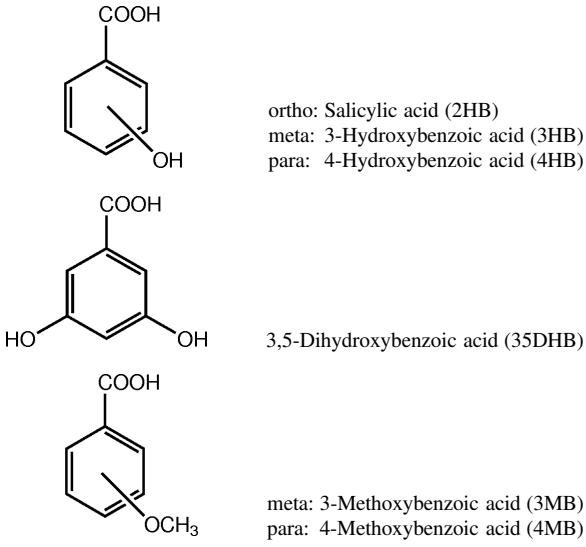

Fig. 2. Chemical structures of the model ligands investigated.

species in a sample as well as the stoichiometry and geometry of the complexes can be obtained. The usefulness of this approach was demonstrated in a recent paper where the FLN technique was applied to Eu(III)-doped glasses [23].

First, spectra of Eu(III) with hydroxy- and methoxybenzoic acids (see Fig. 2) as model ligands for HS are investigated. The obtained ultra-low-temperature luminescence spectra are subsequently compared with those of Eu(III)-HS complexes, and conclusions are drawn regarding binding substructures in HS.

2. Experimental

2.1. Chemicals

Europium(III) chloride ($EuCl_3 \cdot 6H_2O$) was used as luminescence probe. As model compounds for binding sites in HS different aromatic hydroxy- and methoxybenzoic acids were investigated: 2-hydroxybenzoic acid (salicylic acid, 2HB), 3-hydroxybenzoic acid (3HB), 4-hydroxybenzoic acid (4HB), 3,5-dihydroxybenzoic acid (35DHB), 3-methoxybenzoic acid (3MB), 4-methoxybenzoic acid (4MB). The chemicals were purchased from Aldrich with the highest purity available and used as received. HS were isolated according to the IHSS standard procedure from the Gorleben aquifer and separated into fulvic acid (FA) and humic acid (HA) fractions. The basic data on the FA and HA samples can be found in [24]. The FA sample, denoted as GoHy 573 FA, was analyzed in this work. The proton exchange capacity of FA was determined to be (6.8 ± 0.04) meq/g [24]. Stock solutions were prepared in deionized water and the pH value was adjusted to 5 ± 0.5 using HCl or NaOH, as required. The concentration of the stock solutions was 10^{-1} M in case of Eu(III) and the aromatic benzoic acid derivatives. In the case of HS, an 88 g/L stock solution of GoHy 573 FA was prepared. Certain amounts of Eu(III) and ligand stock solutions were mixed to give the required molar ratios. After mixing, the samples were allowed to equilibrate for a minimum time of 3 h at 20 °C based on results obtained from HS fluorescence quenching experiments. Between the measurements the samples were stored in the dark at room-temperature.

2.2. Instruments

For FLN spectroscopy, up to four sample solutions were transferred to quartz tubes (40 mm length × 4 mm o.d. × 2 mm i.d.; volume ca. 100 μL), sealed with rubber septums and cooled simultaneously to 4.7 K in a lab-built sample holder, mounted on a closed-cycle helium refrigerator (SRDK-205 cryostat; Janis Research Company, Wilmington, MA, USA). The samples were excited using a dye laser (LPD 3002; Lambda Physik, Göttingen, Germany) pumped by a XeCl excimer laser (LPX 110i; Lambda Physik). The excitation wavelength was varied between 577 nm and 581 nm using Coumarin 153 (Radiant Laser Dyes & Accessories GmbH, Wermelskirchen, Germany) as laser dye. The laser was operated at 20 Hz with a pulse width of 10 ns. The Eu(III) emission was collected at an angle of 90° angle to the excitation light by two 10 cm F/4 quartz lenses and focused on the entrance slit of a triple monochromator (Spex 1877; Edison, NJ, USA). For detection an intensified iCCD camera (iStar DH720-25U-03; Andor Technologies, Belfast, Northern Ireland) was used in the gated mode. The achieved spectral resolution in the emission dimension was 0.1 nm in a total spectral detection window of 36 nm. The Eu(III) emissions of the $^5D_0 \rightarrow {}^7F_1$ and $^5D_0 \rightarrow {}^7F_2$ transitions were measured simultaneously. For wavelength calibration a neon arc lamp was used. In order to obtain adequate stray light suppression, delay (δt) and gate (Δt) width of the iCCD camera were set to $\delta t = 1.5$ μs and $\Delta t = 10$ ms, respectively.

High-resolution total luminescence spectra (TLS) [25] were constructed by combining the emission

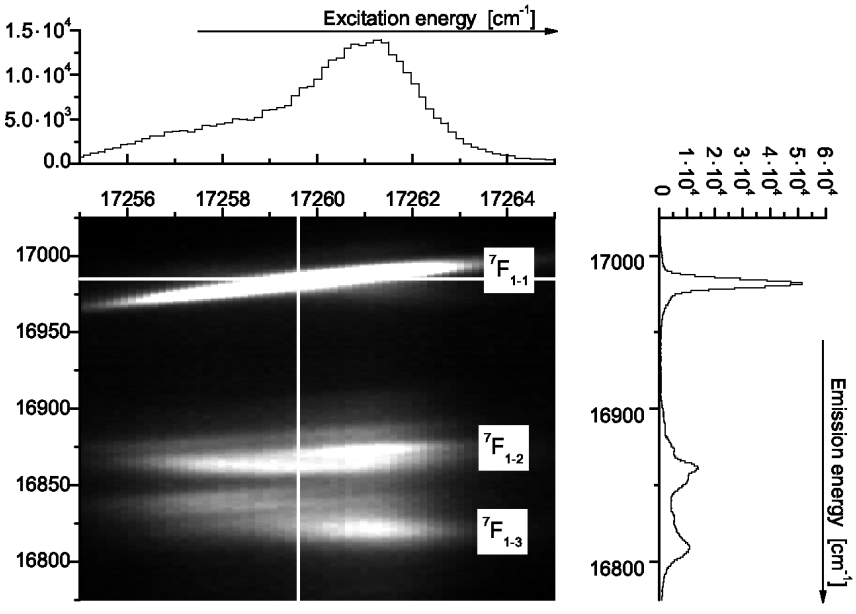

Fig. 3. Contour plot of the $^7F_1$ multiplet of the 1 : 1 Eu(III) : 3MB mixture (for the wavelength range of 588 nm $< \lambda_{em} <$ 596 nm and 579.23 nm $< \lambda_{ex} <$ 579.57 nm). Note the different scales in excitation and emission.

spectra recorded at different excitation wavelengths, using Origin 7.0 software (OriginLab, Northhampton, USA). Each emission spectrum was accumulated over 20 pulses within an 1 s period. The excitation wavelength was varied with a scan rate ranging from 0.001 nm/s to 0.05 nm/s thus defining the resolution in the excitation dimension. All spectra were corrected for the dark current signal of the iCCD camera. The excitation spectra were reconstructed from cross sections of a time series of emission spectra.

3. Results and Discussion

In Fig. 3, a part of the total luminescence spectrum (TLS) of an Eu(III) complex with 3MB is shown. In general, the excitation wavelength was scanned over the spectral range 577 nm $< \lambda_{ex} <$ 581 nm and the luminescence was recorded in the spectral range 585 nm $< \lambda_{em} <$ 621 nm, covering the emission of the $^5D_0 \rightarrow {}^7F_1$ and the $^5D_0 \rightarrow {}^7F_2$ transitions. An enlarged view of the $^5D_0 \rightarrow {}^7F_1$ transition (588 nm $< \lambda_{em} <$ 596 nm, with 579.23 nm $< \lambda_{ex} <$ 579.57 nm) is shown here. For these experiments a major challenge was the extremely low extinction coefficient of the $^5D_0 \leftarrow {}^7F_0$ transition, due to parity forbiddance of the f-f transitions. This forbiddance is relaxed partially in case the symmetry of the Eu(III) complex is lowered, e. g., due to the formation of non-centrosymmetric complexes or due to vibrational motion of the ligands. In Fig. 3 also regular 2-D spectra, emission as well as excitation spectra (right and top, respectively), are shown which can be obtained as cross sections through the TLS (vertical and horizontal lines, respectively). Compared to room-temperature emission spectra, in which the $^5D_0 \rightarrow {}^7F_1$ transition appears as a single broad band of ca. 10 nm FWHM (spectra not shown), the FLN spectra recorded at 4.7 K show greatly improved spectral resolution of the luminescence peaks, in which the Stark levels of the ^7F_J transitions are resolved (see Fig. 3, right, and the illustration below). The Stark levels are a result of the crystal-field, which removes the degeneracy of the $^{(2S+1)}L_J$ levels.

As reference systems the TLS of $EuCl_3 \cdot 6H_2O$ crystals and of an aqueous $EuCl_3$ sample were also measured at 4.7 K. For the $EuCl_3 \cdot 6H_2O$ crystals a single $^5D_0 \leftarrow {}^7F_0$ transition was observed with a very low FWHM of only 0.2 cm^{-1}. For the complexes with organic ligands the $^5D_0 \leftarrow {}^7F_0$ transition was found to be broader: in the range 2 cm^{-1} < FWHM < 23 cm^{-1} depending on the particular ligand. The width of the excitation spectrum of the Eu : 3MB sample in Fig. 3 is ca. 6 cm^{-1}. From the experimental data it can be concluded that in the reference system $EuCl_3 \cdot 6H_2O$ only a single, well-defined Eu(III) complex is present. On the other hand, for the Eu(III) samples with the organic ligands, the broader peaks in excitation and emission already point to the presence of more than one type of complex (= "species"). This is supported by

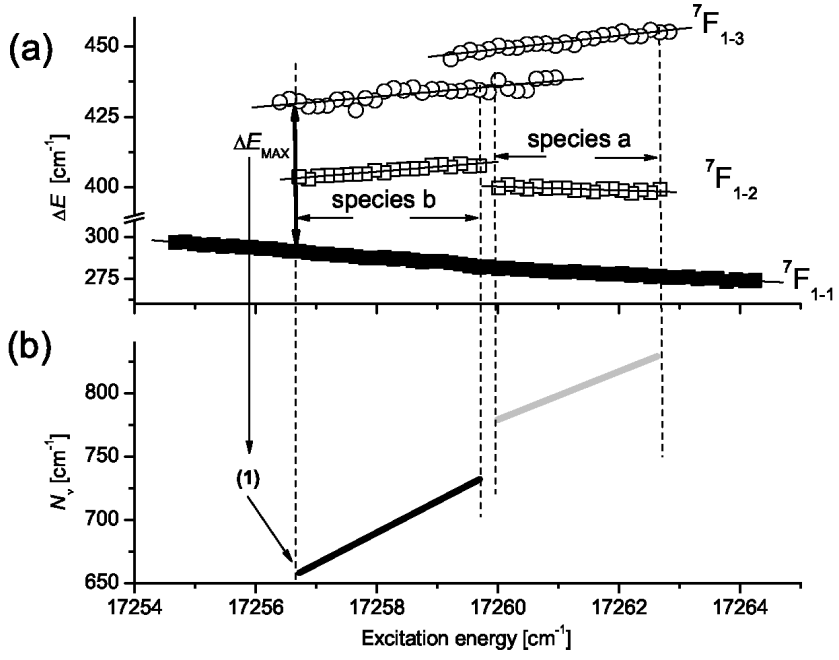

Fig 4. (a) Stark levels of the $^7F_1$ multiplet of the 1 : 1 Eu(III) : 3MB mixture, derived from the emission maxima in the contour plot of Figure 3. The *y*-axis refers to ΔE, the difference with the excitation energy. (b) The *y*-axis now refers to the crystal-field strength parameter N_v, which is calculated from ΔE_{MAX} (energy difference between $^7F_{1-1}$ and $^7F_{1-3}$ for the lowest and the highest excitation energy of a species) according to (1).

the asymmetric shape of the $^5D_0 \leftarrow {}^7F_0$ transition (see Fig. 3, top). In addition, for the second ($x = 2$) and third ($x = 3$) peak of the $^5D_0 \rightarrow {}^7F_{1-x}$ transition, "islands" in the TLS clearly indicate the presence of more than one species.

Furthermore an interdependence of the Stark level energies of the $^5D_0 \rightarrow {}^7F_{1-x}$ ($x = 1,2,3$) (see Fig. 3) as well as of the $^5D_0 \rightarrow {}^7F_{2-y}$ ($y = 1-5$, data not shown) transitions and the excitation wavelength is observed. Especially the shift in the position of the $^5D_0 \rightarrow {}^7F_{1-1}$ transition upon scanning the excitation wavelength is most evident. The relatively narrow, sloping lines (instead of broad, oval-shaped peaks) indicate, that the energies of the $^5D_0 \leftarrow {}^7F_0$ and the $^5D_0 \rightarrow {}^7F_{1-x}$ transitions in the inhomogeneously broadened sample are correlated [26]. From the different slopes it can clearly be seen that the observed shifts are different for the three Stark levels of the $^5D_0 - {}^7F_1$ transition.

In order to visualize the dependence on the excitation wavelength, the energy difference ΔE between the $^5D_0 \leftarrow {}^7F_0$ excitation and the maxima of the $^5D_0 \rightarrow {}^7F_{1-x}$ ($x = 1,2,3$) emission bands was calculated. It should be noted that in contrast to conventional molecular FLN spectroscopy, in which vibronic excitation/emission takes place within the same electronic transition and ΔE is constant for a specific vibration, for these systems ΔE was found to be intercorrelated with E_{ex} and to be different for the various $^7F_{1-x}$ levels; the variation in slopes is clearly shown in Figure 4a. A similar dependence has been reported for the luminescence of Eu(III) in glassy matrices [23, 27]. The slight, continuous changes in ΔE can be attributed to slight differences in the further environment of the complexes, e. g., to slight difference in (i) bond lengths, (ii) angles between ligands, or (iii) in the second coordination sphere, whereas abrupt discontinuities in the slope point towards larger differences in the first coordination sphere, in particular different coordination numbers of organic ligands and/or of water molecules are observed. Consequently, this may involve larger differences in the symmetry. Therefore, the latter phenomena were attributed to different "species" [20, 28]. In Fig. 3 the different Eu(III) : 3MB species can be seen as "islands" in the emission range 592 nm $< \lambda_{\mathrm{em}} <$ 596 nm. Depending on the sample, different numbers of such species were found (see Figs. 5 and 6).

For weak crystal-fields (1) connects ΔE_{MAX}, the energy difference between $^7F_{1-1}$ and $^7F_{1-3}$ for the lowest and the highest excitation energy of a species (see Fig. 4a), to the crystal-field strength parameter $N_v(\mathrm{B_{2q}})$ [29, 30]:

$$N_v(\mathrm{B_{2q}}) = \sqrt{\frac{\pi(2+\alpha^2)}{0.3}}\Delta E_{\mathrm{MAX}}, \quad \text{with } \alpha = \frac{E_{\mathrm{b}} - E_{\mathrm{C}}}{\Delta E_{\mathrm{MAX}}/2}, \tag{1}$$

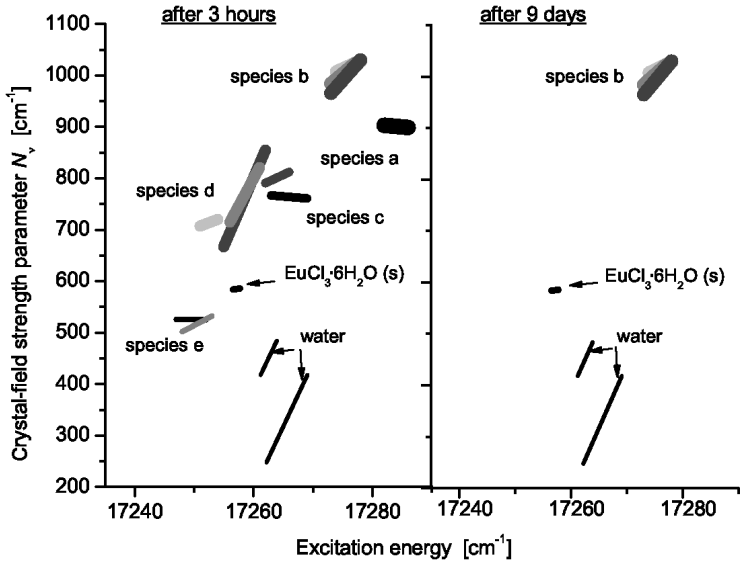

Fig. 5. Crystal-field strength parameters of the various Eu(III) species in 2HB samples, in water, and in solid $EuCl_3 \cdot 6H_2O$. After nine days of storage, the Eu : 2HB samples showed only a single species b.

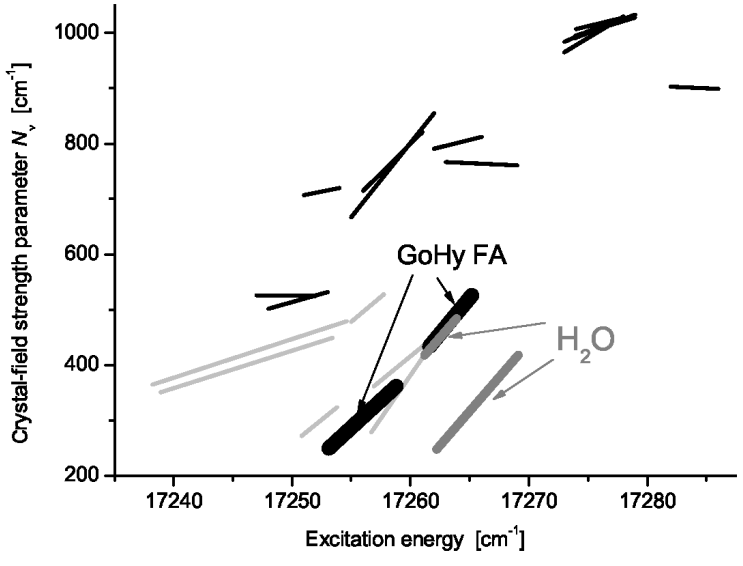

Fig. 6. Crystal-field strength parameters of Eu(III)-HS complexes (black, bold) in comparison with those observed in water (dark grey, semi-bold), 2HB samples (black), and 3HB samples (light grey), the latter being representative for non-chelating hydroxybenzoates.

where E_b is the energy of the barycentre of the $^7F_1$ multiplet (mean energy) and E_C is the energy of the central level. Calculating $N_v(B_{2q})$ for the lowest and highest ΔE_{MAX} of each species and plotting it versus the excitation energy, a graph such as in Fig. 4b is obtained, which allows the comparison of the complexes formed in different Eu(III)-ligand systems based on their different crystal-field strengths.

In Fig. 5 the crystal-field strength parameter $N_v(B_{2q})$ vs. excitation energy is shown for salicylic acid (2HB) at different Eu(III) : 2HB ratios. Compared to other hydroxybenzoic acid complexes investigated, 2HB shows a larger $N_v(B_{2q})$ value, which was found to be in the range 500 $cm^{-1} < N_v(B_{2q}) <$ 1000 cm^{-1}, and also a slightly higher excitation energy, which was found to be in the range 17250 cm^{-1} (579.7 nm) $< E_{ex} <$ 17285 cm^{-1} (578.5 nm). For the Eu(III) complexes with *meta*- and *para*-hydroxybenzoic acids smaller crystal-field strength parameters of 200 $cm^{-1} < N_v(B_{2q}) <$ 500 cm^{-1} were observed, as shown in Fig. 6 for 3HB. The large $N_v(B_{2q})$ value was attributed to the formation of chelates between 2HB and Eu(III) in which the concentration of nega-

tive charges close to the Eu(III) ion is suggested to be higher. *Meta*- and *para*-hydroxybenzoic acids are not capable of forming chelate complexes due to structural constraints.

As a reference, also the data obtained for $EuCl_3 \cdot 6H_2O$ crystals and for an aqueous sample of $EuCl_3$ (both measured at 4.7 K) are shown. For both samples the observed $N_\nu(B_{2q})$ dependence on the excitation energy was significantly different from the Eu-ligand systems, providing an important confirmation of the actual complex formation between Eu(III) and the organic ligands.

For the first time also TLS of Eu(III) complexed to HS were recorded and evaluated according to the methods described before (vide supra). In Fig. 6 the dependence of the crystal-field strength parameter $N_\nu(B_{2q})$ on the excitation energy is shown for Eu(III) complexed to HS (GoHy 573 FA, bold lines) and compared to the data found for the model compounds and reference systems investigated. Two conclusions may be drawn from the observed tendencies: 1) In HS the tendency of formation of chelates – if any – seems to be very small, i. e. the major binding is achieved via interaction comparable to complexes formed with carboxylic acids that are not capable of chelate formation, e. g., *meta*- and *para*-substituted benzoic acids. Complexes of the GoHy 573 FA seem to be similar to 3- or 4-hydroxybenzoic acid or 3,5-dihydroxybenzoic acid, but not to salicylate complexes as often presumed [19]. In other words, the binding sites in the fulvate do not seem to form chelates as major binding form but nevertheless the binding is accomplished via deprotonated carboxylate groups. 2) A large fraction of the Eu(III) ions doesn't seem to be complexed since the observed $N_\nu(B_{2q})$ value is very similar to that of the aqueous reference sample. This could be explained by the excess of Eu(III) in this sample. The assumption, that upon binding to HS outer-sphere complexes are formed initially and a possible formation of inner-sphere complexes needs more time, could also be important here. In room-temperature experiments, in which the quenching of the intrinsic HS fluorescence upon addition of lanthanoide ions was measured in a stopped-flow set up, the complexation reaction (measured as effective HS fluorescence quenching) occurred on a millisecond to second time scale. The HS samples used in the low-temperature measurements were equilibrated with Eu(III) for one day. It was expected that this time span is sufficient to reach equilibrium.

On the other hand in storage experiments with model ligands, e. g., 2HB, a significant influence of the equilibration time was observed. In Fig. 5 the observed influence of the equilibration time between 2HB and Eu(III) on $N_\nu(B_{2q})$ is shown. Initially, for 2HB a larger number of species was identified, but upon storage of the samples for nine days at 20 °C the different species merged into a single one. This indicates that the initially formed complexes are subject to relatively slow reorganization processes until only the thermodynamically stable form remains. For 2HB a maximum change in the $N_\nu(B_{2q})$ value of $\sim 500\ cm^{-1}$ was observed (see Fig. 5). A similar observation, but to a much smaller extent, has been made concerning 3MB-complexes. Small changes in the $N_\nu(B_{2q})$ value of about $50\ cm^{-1}$ to $60\ cm^{-1}$ after 20 h of storage at room-temperature were found here. Although 2HB and 3MB are only small ligands, some time is apparently needed for the formation of the thermodynamically stable complexes. It is attractive to assume that for larger ligands like in the case of HS even longer equilibration times might be necessary to reach equilibrium, which would be contrary to the results of the room-temperature fluorescence quenching experiments. Work is in progress to further investigate this effect.

The number of Stark levels that can be observed in the luminescence spectra is dependent on the point symmetry group of the coordination polyhedron that is formed between Eu(III) and the ligands. Depending on the symmetry, different patterns of Stark levels can be observed for the $^5D_0 \rightarrow {}^7F_1$ and the $^5D_0 \rightarrow {}^7F_2$ transitions. In Fig. 7 the luminescence spectra recorded at 4.7 K for Eu(III) with different benzoic acids and of solid $EuCl_3 \cdot 6H_2O$ are compared. It can be seen that the number of observed Stark levels is dependent on the specific ligand and species, indicating the formation of complexes with different symmetries. In case the $^5D_0 \rightarrow {}^7F_1$ transition is split into three lines, the possible point groups are D_2, C_{2v} (orthorhombic), C_2, C_s (monoclinic) or C_1 (triclinic). Further discrimination is carried out based to the splitting of the $^5D_0 \rightarrow {}^7F_2$ transition: three lines $\rightarrow D_2$; four lines $\rightarrow C_{2v}$; five lines $\rightarrow C_s$, C_1 or C_2. The latter case can only be further distinguished by polarization measurements [31].

The luminescence spectra of the $^5D_0 \rightarrow {}^7F_1$ and the $^5D_0 \rightarrow {}^7F_2$ transitions of the different species for each model ligand and for HS were evaluated with respect to the number of Stark levels visible in the spectrum. For a particular ligand different complex symmetries were found depending on the species at hand, e. g., for

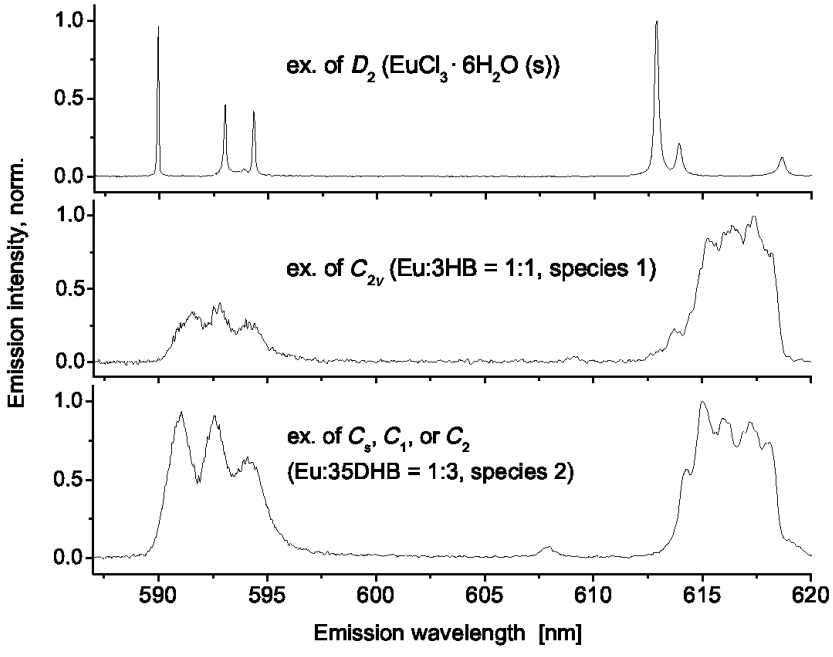

Fig. 7. Examples of emission spectra illustrating the assignment of point groups depending on the number of transitions in the emission spectrum (see text).

2HB a C_{2v} symmetry was attributed to the species a and b while a C_u symmetry ($u = s$, 1 or 2) was assigned to the species c, d, and e, respectively (see also Fig. 5). In general, for the model ligands and for HS all complexes showed a C_z symmetry ($z = 2v$, s, 1 or 2), while the reference samples showed a higher symmetry, D_2.

4. Summary

FLN spectra of Eu(III) complexes with different hydroxybenzoic acids and HS were recorded in frozen aqueous solutions at 4.7 K. The complexes were excited directly in the $^5D_0 \leftarrow {}^7F_0$ transition, and the non-degeneracy of this transition was used for the selective excitation and subsequent identification of the different complexes formed between Eu(III) and the ligands investigated. In the jackstraws plots of the various species, an interdependency of excitation energy and crystal-field strength was observed, which cannot be fully explained by only considering Coulomb forces of the crystal-field or the symmetry of the complexes (e. g., see Fig. 5 and 6).

The comparison of Eu(III) spectra recorded in the presence of HS and model compounds indicates that in HS under the experimental conditions applied the dominant binding is achieved via the carboxylate groups of HS [32]. A contribution from hydroxy groups like in salicylic acid, which forms complexes of the chelate type, could not be detected. For HS the experiments further showed that the preferred complex symmetry seems to be C_{2v}. Based on the observations with salicylic acid and 3MB, the formation of the thermodynamically stable complexes of Eu(III) is rather slow and thus may take several days, which has also been reported for other organic ligands [33]. It can be expected that for larger molecules like HS the formation of the thermodynamically stable complexes is even slower, most likely due to structural reorientations of the HS. Work is in progress to further investigate this phenomenon.

Acknowledgement

The authors are thankful to Gunnar Buckau and Manfred Wolf for the supply of the HS samples. The work was financially supported by the BMWi (contract no. 02E10216) and by the European Commission (Access to Research Infrastructures Action of the Improving Human Potential Program, contract no. RII-CT-2003-506350, LCVU grant 001124).

[1] G. E. Batley, S. C. Apte, and J. L. Stauber, Aus. J. Chem. **57**, 903 (2004).
[2] T. H. Christensen and D. L. Baun, Waste Manage. Res. **22**, 3 (2004).
[3] G. Barancikova and J. Makovnikova, Plant, Soil and Environment **49**, 565 (2003).
[4] G. Davies, E. A. Ghabbour, and C. Steelink, J. Chem. Educ. **78**, 1609 (2001).
[5] M. D. Hays, D. K. Ryan, and S. Pennell, Anal. Chem. **76**, 848 (2004).
[6] www.funmig.com (last access 17.09.08)
[7] F. H. Frimmel, G. Abbt-Braun, K. G. Heumann, B. Hock, and H.-D. Lüdemann, in: Refractory Organic Substances (ROS) in the Environment (Ed. M. Spiteller), John Wiley & Sons, New York 2002.
[8] V. Moulin and C. Moulin, Radiochim. Acta **89**, 773 (2001).
[9] F. J. Stevenson, Humus Chemistry – Genesis, Composition, Reactions, Wiley VCH, Weinheim 1982.
[10] R. Sutton and G. Sposito, Environ. Sci. Technol. **39**, 9009 (2005).
[11] D. K. Ryan and J. H. Weber, Anal. Chem. **54**, 986 (1982).
[12] F. Ariese, S. van Assema, C. Gooijer, A. G. Bruccoleri, and C. H. Langford, Aquat. Sci. **66**, 1 (2004).
[13] F. S. Richardson, Chem. Rev. **82**, 541 (1982).
[14] J.-C. G. Bünzli, in: Lanthanide Probes in Life, Chemical and Earth Science (Eds. J.-C. G. Bünzli and G. R. Choppin), Elsevier Science Publishers BV, Amsterdam 1989, p. 219.
[15] J. W. Thomason, W. Susetyo, and L. A. Carreira, Appl. Spectrosc. **50**, 401 (1996).
[16] M. U. Kumke, S. Eidner, and T. Krüger, Environ. Sci. Technol. **39**, 9528 (2005).
[17] G. Plancque, Y. Maurice, V. Moulin, P. Toulhoat, and C. Moulin, Appl. Spectrosc. **59**, 432 (2005).
[18] W. T. Carnall, in: Handbook of Physics and Chemistry of Rare Earths (Eds. K. A. Gschneidner, Jr. and L. Eyring), North-Holland Publishing Company, Amsterdam 1979, p. 171.
[19] T. H. Yoon, H. Moon, Y. J. Park, and K. K. Park, Environ. Sci. Technol. **28**, 2139 (1994).
[20] H. S. Shin and G. R. Choppin, Radiochim. Acta **86**, 167 (1999).
[21] R. Jankowiak, in: Chemical Analysis Series, Vol. 156 – Shpol'skii Spectroscopy and Other Site-Selection Methods (Eds. C. Gooijer, F. Ariese, and J. W. Hofstraat), John Wiley & Sons, New York 2000.
[22] M. U. Kumke, F. H. Frimmel, F. Ariese, and C. Gooijer, Environ. Sci. Technol. **34**, 3818 (2000).
[23] V. Venkatramu, D. Navarro-Urrios, P. Babu, C. K. Jayasankar, and V. Lavín, J. Non-Cryst. Solids **351**, 929 (2005).
[24] M. Wolf, G. Buckau, and S. Geyer, in: Humic Substances in Performance Assessment of Nuclear Waste Disposals: Actinoide and Iodine Migration in the Far-Field (Vol. FZKA6969), Forschungszentrum Karlsruhe 2004, p. 111.
[25] J. W. Hofstraat and U. P. Wild, in: Chemical Analysis Series, Vol. 156 – Shpol'skii Spectroscopy and Other Site-Selection Methods (Eds. C. Gooijer, F. Ariese, and J. W. Hofstraat), John Wiley & Sons, New York 2000.
[26] E. Antic-Fidancev, J. Alloys Compd. **300 – 301**, 2 (2000).
[27] G. Boulon, M. Bouderbala, and J. Sériot, J. Less-Comm. Met. **112**, 41 (1985).
[28] J. P. Jouart and G. Mary, J. Lumin. **44**, 193 (1989).
[29] V. Lavín, P. Babu, C. K. Jayasankar, I. R. Martín, and V. D. Rodríguez, J. Chem. Phys. **115**, 10935 (2001).
[30] O. L. Malta, E. Antic-Fidancev, M. Lemaitre-Blaise, A. Milicic-Tang, and M. Taibi, J. Alloys Compd. **228**, 41 (1995).
[31] C. Görller-Walrand and K. Binnemans, in: Handbook of Physics and Chemistry of Rare Earths, Vol. 23 (Eds. K. A. Gschneidner, Jr. and L. Eyring), Elsevier Science Publishers BV, Amsterdam 1996, p. 121.
[32] M. E. Azenha, H. D. Burrows, S. M. Fonseca, M. L. Ramos, J. Rovisco, J. S. de Melo, A. J. F. N. Sobral, and K. Kogej, New J. Chem. **32**, 1531 (2008).
[33] J.-C. G. Bünzli, in: Metal Ions in Biological Systems (Eds. A. Sigel and H. Sigel), Marcel Dekker, New York, Basel 2001, p. 39.